Observations of atmospheric tides on Mars at the season and latitude of the Phoenix atmospheric entry

Paul Withers[1] and D. C. Catling[2]

Received 2 September 2010; revised 22 October 2010; accepted 28 October 2010; published 23 December 2010.

[1] We report on the atmospheric structure derived from atmospheric entry of NASA's Phoenix Mars probe using Phoenix Atmospheric Structure Experiment (ASE) data complemented by Mars Climate Sounder (MCS) temperature-pressure profiles. Oscillations in temperature, caused by thermal tides, have vertical wavelengths of tens of kilometres. Their amplitudes are much larger in individual profiles than in dayside and nightside zonal mean MCS profiles which is inconsistent with sole control by the migrating diurnal tide. In the fixed local time reference frame of dayside MCS observations, temperature varies by >15 K with longitudinal wavenumber 3, which could arise from non-migrating tides produced by the interaction of surface topography with the migrating diurnal tide. **Citation:** Withers, P., and D. C. Catling (2010), Observations of atmospheric tides on Mars at the season and latitude of the Phoenix atmospheric entry, *Geophys. Res. Lett.*, *37*, L24204, doi:10.1029/2010GL045382.

1. Introduction

[2] Phoenix [*Smith et al.*, 2009] was launched on 4 August 2007 and landed on Mars in the late afternoon (16.6 hrs local true solar time) in the Vastitas Borealis region (68.2°N, 234.2°E, −4131 m elevation) at a UTC time of 23:38 on 25 May 2008 (L_s = 76.6°) (Table 1). Data from its entry, descent, and landing (EDL) have been used to obtain a profile of martian atmospheric density, pressure, and temperature from ~13.5 km to ~130 km above ground level. This is the first such profile of atmospheric structure from the martian polar regions. The thermal structure of the martian atmosphere is sensitive to radiative forcing from suspended dust and to diabatic heating associated with atmospheric dynamics [*Zurek et al.*, 1992; *Leovy*, 2001]. It is also perturbed by a wide variety of waves and tides. Here we report the identification of the effects of atmospheric tides in the Phoenix atmospheric entry profile, when examined in the context of near-contemporaneous orbital remote sensing by the Mars Climate Sounder (MCS) instrument on Mars Reconnaissance Orbiter (MRO) [*McCleese et al.*, 2007]. We begin with the Phoenix temperature profile, compare it to a single MCS profile from similar time, latitude, longitude, and season, explore the differences between these two individual profiles and zonal mean MCS profiles, and investigate the importance of longitude for influencing atmospheric conditions.

[3] The Phoenix Atmospheric Structure Experiment (ASE) recorded accelerometer and gyroscope data during entry, from which *Withers et al.* [2010] derived a vertical profile of atmospheric density, pressure, and temperature. The atmospheric profile and documentation of the data reduction and processing are available at the NASA Planetary Data System (PDS) [*Withers et al.*, 2010]. Results shown in this paper are based on "compact" profiles archived at 1 km vertical resolution.

[4] Figure 1a shows the Phoenix temperature profile. All altitudes reported in this paper, including the axis in Figure 1a, are referenced to the ground level at the landing site, whose radial distance as shown in Table 1 is 3376.3 km [*Withers et al.*, 2010], instead of to an equipotential surface defined by the Mars Orbiter Laser Altimeter (MOLA) [*Smith et al.*, 2003]. The mesopause is clearly observable in Figure 1a at 128.4 ± 1.7 K, (5.2 ± 1.8) × 10^{-3} Pa, and 102 ± 2 km, where these 1σ uncertainties were found using a bootstrap error estimation technique on data between 90 and 110 km. The growing importance of extreme ultraviolet heating over infrared cooling above the mesopause is evident as a temperature rise with increasing altitude. Several cycles of wave-like oscillations in temperature, which are the focus of this work, are present between 30 and 80 km. Atmospheric dust loading affects thermal structure at lower altitudes and the Phoenix Surface Stereo Imager (SSI) determined that the local visible optical depth on Phoenix sol 0 was 0.28–0.65 at a 95% confidence level, with a most probable value of 0.39 (M. Lemmon, personal communication, 2010). The mean lapse rate between 20 km and 30 km is 1.5 ± 0.3 K km^{-1}, smaller than the dust-free adiabatic lapse rate of 4.5 K km^{-1}.

[5] We interpret the temperature oscillations between 30 and 80 km in Figure 1a as being caused by thermal tides. Thermal tides are global-scale oscillations in atmospheric state variables, such as density, pressure and temperature, that are driven by periodic solar forcing [*Chapman and Lindzen*, 1970; *Forbes*, 1995]. They are particularly prominent on Mars due to its rapid rotation rate and the low atmospheric density at its surface [*Zurek*, 1976; *Wilson and Hamilton*, 1996; *Zurek et al.*, 1992; *Banfield et al.*, 2000, 2003]. Since the direct solar forcing can be represented as a series of terms whose frequencies are integer multiples of the reciprocal of the length of the martian solar day (diurnal, semi-diurnal, ter-diurnal, etc. terms), thermal tides are limited to the same set of temporal frequencies. Diurnal and semi-diurnal terms are typically dominant. Tidal oscillations are also restricted in how they may vary with longitude. They must contain an integer number of cycles per

[1]Center for Space Physics, Boston University, Boston, Massachusetts, USA.
[2]Department of Earth and Space Sciences, University of Washington, Seattle, Washington, USA.

0094-8276/10/2010GL045382

Table 1. Time and Position of Phoenix Landing

Time[a] (UTC)	2008-05-25T23:38:24
Aerocentric latitude[b] (°N)	68.21878 ± 0.00006
Longitude[b](°E)	234.24845 ± 0.000096
Radius[b](km)	3376.2915 ± 0.0014
Elevation[c](m)	−4131
L_s[d](degrees)	76.6
Local true solar time[e](hrs)	16.6

[a]*Smith et al.* [2009].
[b]Martin-Mur (personal communication, 28 May 2008). The landed latitude, longitude and radius, which are shown with 1σ uncertainties, were determined from Doppler tracking.
[c]Elevation is with respect to the areoid defined by the Mars Orbiter Laser Altimeter (MOLA) investigation, specifically 16 pixels per degree gridded MOLA data acquired from http://geo.pds.nasa.gov/missions/mgs/megdr.html [*Smith et al.*, 2003].
[d]Calculated using http://www-mars.lmd.jussieu.fr/mars/time/martian_time.html.
[e]Calculated from tabulated time and position using SPICE tools provided by JPL's Navigation and Ancillary Information Facility (NAIF).

360°. Accordingly, any tidal oscillation can be represented as [*Forbes et al.*, 2002]:

$$\sum_n \sum_s A_{n,s}(z,\theta)\cos\big(n\Omega t + s\lambda - \phi_{n,s}(z,\theta)\big) = \sum_n \sum_s A_{n,s}(z,\theta)\cos\big(n\Omega t_{LST} + (s-n)\lambda - \phi_{n,s}(z,\theta)\big) \quad (1)$$

where A is an amplitude, z is altitude, θ is latitude, n is a non-negative integer, Ω is the planetary rotation rate, t is universal time, s is an integer, λ is east longitude and ϕ is a phase. Equation (1) uses $\Omega t = \Omega t_{LST} - \lambda$, where t_{LST} is local solar time. Tidal components that have $s = n$ are "migrating" tides and those that do not are "non-migrating" tides. Migrating tides are produced directly by solar heating and non-migrating tides are produced indirectly by the interaction of solar forcing with zonally asymmetric conditions, usually surface topography. In an idealized atmosphere, a given s, n tidal oscillation is the sum of multiple tidal (or Hough) modes. Each tidal mode has a characteristic latitudinal and vertical structure. The vertical wavelength depends on the background scale height, the static stability, and an "equivalent depth" that is a unique lengthscale associated with each

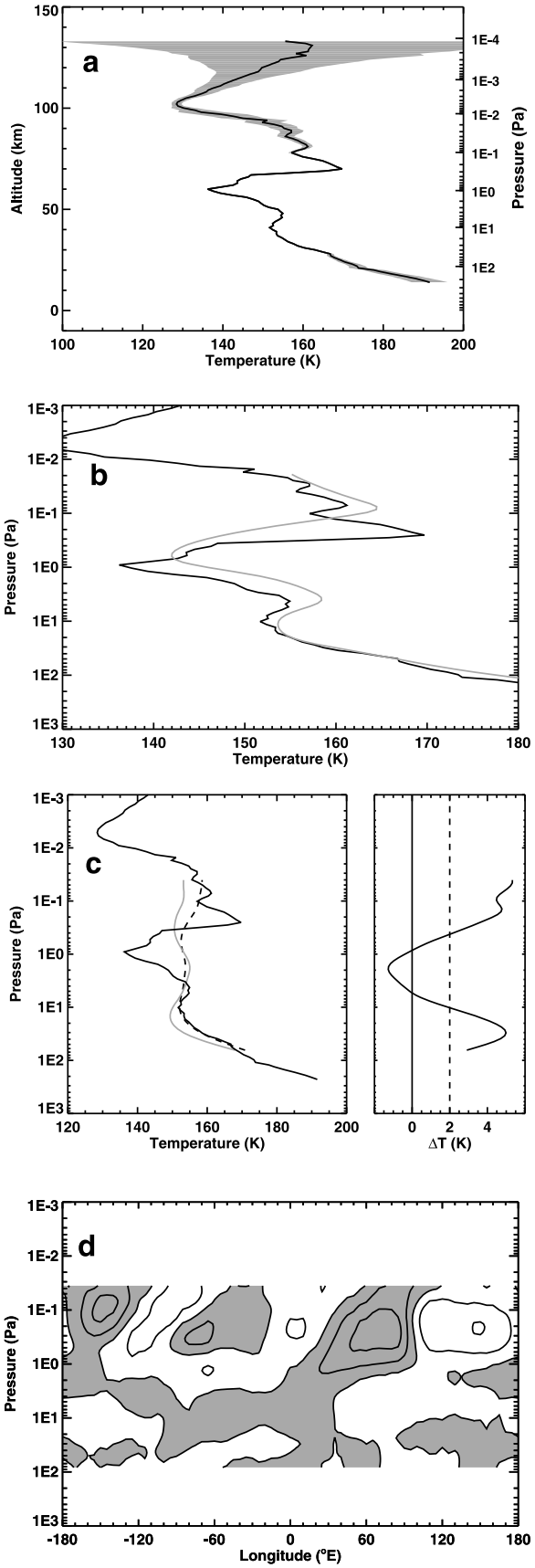

Figure 1. (a) Vertical profile of reconstructed temperature for Phoenix (black solid line), with 1σ temperature uncertainties shown by the grey envelope. (b) Phoenix temperature profile (black solid line) and an MCS temperature profile (grey solid line) obtained at similar latitude and longitude two hours earlier in local time and universal time. (c) (left) Phoenix temperature profile (black solid line), zonal mean dayside MCS temperature profile (black dashed line), and zonal mean nightside MCS temperature profile (grey solid line). (right) Difference between zonal mean dayside and nightside MCS profiles (curved black line). Temperature differences of 0 K and 2 K are marked by the vertical solid and dashed lines, respectively, where the latter is the average difference between dayside and nightside MCS profiles. (d) Contour plot of the difference between dayside MCS temperature profiles from 25 May to 4 June 2008 and a zonal mean temperature profile. Contour intervals are at −8, −4, 0, 4 and 8 K. Positive temperature differences are shaded grey.

tidal mode [e.g., *Magalhães et al.*, 1999]. Non-migrating tides, but not migrating tides, can cause variations with longitude in a fixed local time reference frame. Migrating tides are dominant near the surface [*Zurek et al.*, 1992] and non-migrating tides are strong in the thermosphere [*Withers et al.*, 2003], but their properties and behaviour in the "transition zone" of the middle atmosphere are not well-known from observations.

2. Analysis and Results

[6] Identification of the specific tidal modes responsible for the temperature oscillations in a single profile, such as the Phoenix temperature profile, is challenging. Conveniently, MCS made complementary atmospheric observations in the days surrounding the Phoenix atmospheric entry. MCS is an filter radiometer that retrieves vertical $T(p)$ profiles between the surface and $p \approx 0.03$ Pa from infrared observations of limb radiances [*Kleinböhl et al.*, 2009]. MCS data products from May and June 2008 are available online at http://atmos.nmsu.edu/PDS/review/MROM_2021/ and MROM_2022/(part of dataset MRO-M-MCS-5-DDR-V1.0). We used data from files 2008MMXXHH_DDR.TAB, where MM is 05 (May) or 06 (June), XX is the two digit day of the month, and HH = 00, 04, 08, 12, 16, 20, in PDS volumes MROM_2021 and MROM_2022. MCS profiles cover all latitudes and two local solar times (LSTs, nominally 3 AM and 3 PM). We therefore built up a more complete picture of the atmospheric state at the latitude and season of the Phoenix atmospheric entry (68.2°N and L_s = 76.6°) by using data from both MCS and Phoenix, thereby sampling the atmosphere at a range of longitudes and two LSTs.

[7] On 25 May 2008, MCS acquired a $T(p)$ profile directly above the Phoenix landing site at a UTC time of 21:38 (two UTC hours prior to Phoenix entry), 68.3°N, 234.5°E, and 14.6 hours LST (two LST hours prior to Phoenix entry). Figure 1b compares this individual MCS profile to the Phoenix temperature profile. Several cycles of wave-like oscillations in temperature, most likely caused by thermal tides and waves, are present in both profiles. The overall thermal structure is similar in both profiles, although the temperatures and pressure levels of the two sets of temperature extrema are not identical. The temperatures and pressures of the four main temperature extrema in the Phoenix temperature profile are 10 Pa and 152 K, 4.3 Pa and 155 K, 0.91 Pa and 136 K, and 0.25 Pa and 170 K. Corresponding values for MCS are 11 Pa and 154 K, 4.1 Pa and 158 K, 0.63 Pa and 142 K, and 0.075 Pa and 164 K.

[8] We sought to identify the tidal mode(s) responsible for these wave-like oscillations. Surface pressure variations observed by Phoenix after landing are dominated by the diurnal migrating tide, which is often a strong component of periodic atmospheric disturbances on Mars, but also show the effects of other modes with different frequencies [*Taylor et al.*, 2010]. The diurnal migrating tide has a vertical wavelength of 24 km or 3 scale heights, using a scale height of ~8 km [*Magalhães et al.*, 1999]. Although this is consistent with the spacing of some of the Phoenix and MCS temperature extrema in Figure 1b, it is not consistent with the spacing of all extrema. Also, dominance by the diurnal migrating tide does not explain why the ratio of MCS pressure at a temperature extremum to the corresponding Phoenix pressure decreases from 1.1 (11 Pa/10 Pa) at the lowest altitude to 0.3 (0.075 Pa/0.25 Pa) at the highest altitude. Two possible reasons for these discrepancies are the non-vertical trajectory of Phoenix and Phoenix-MCS local time/longitude differences. The local time (16.6 hours) and longitude (234.2°E) stated previously for Phoenix correspond to the landing site. Phoenix traveled eastward by 30 degrees, and the local time at the spacecraft increased by two hours, between the mesopause and landing. So the local time at the 0.25 Pa/170 K maximum (70 km) in the Phoenix temperature profile is very close to the 14.6 hours of Figure 1b's MCS profile, while the longitude of this feature in the Phoenix temperature profile is tens of degrees west of the corresponding feature in Figure 1b's MCS profile. These possible reasons cannot resolve all discrepancies, leaving the conclusion that the atmosphere at this latitude and season is not solely dominated by the diurnal migrating tide.

[9] We investigated the dynamical state of the atmosphere at this latitude and season further by considering more MCS data. Figure 1c shows zonal mean MCS temperature profiles from the dayside and nightside of Mars. Figure 1c contains all MCS profiles from 25 May to 4 June, inclusive, whose latitudes were within 2 degrees of the Phoenix landing site. Their local times were either 14.4–14.8 hours (dayside) or 3.4–3.8 hours (nightside). Wave-like oscillations are again present, but with much smaller amplitudes than in the individual Phoenix and MCS profiles in Figure 1b. If the diurnal migrating tide were the only atmospheric oscillation present, the amplitude would be similar in the zonal-mean profile and individual profiles. The difference between the zonal mean dayside and nightside MCS profiles, which is also shown in Figure 1c, oscillates with altitude as well. Allowing for a 2 K difference in average temperature between dayside and nightside, the amplitude of these temperature differences is ±3 K at all altitudes. The three extrema in temperature difference are 5.0 K at 30 Pa, −1.3 K at 1.9 Pa, and 4.8 K at 0.14 Pa. The altitude differences between adjacent extrema, which equal half the vertical wavelength of the underlying disturbance, are 20–22 km, assuming a scale height of ~8 km. The diurnal migrating tide has the appropriate period to account for these day-night differences, but its vertical wavelength is too short by a factor of two.

[10] Figure 1d shows how dayside MCS temperature profiles vary with longitude. Only non-migrating tides can cause variations with longitude in this fixed local time reference frame. At pressures smaller than about 1 Pa, strong and regular variations in temperature with longitude are apparent, dominated by a harmonic component with three cycles per 360° of longitude (wave-3). The temperature at 0.3 Pa is 166 K at 75°E, but 148 K at 110°E, which is a difference of 18 K over only 35 degrees of longitude (800 km). This is much greater than the 4 K difference between the zonal mean dayside and nightside MCS temperatures at this pressure level, which emphasizes the significance of these variations in longitude. This is also quite distinct from the behaviour given by *Lee et al.* [2009, Figure 1] where variations with longitude in MCS temperatures (45°N–50°N, L_s = 156°–162°) are smaller (10 K) than the day-to-night difference (20 K). The phase of the longitudinal structure in Figure 1d moves eastward by about 60° as pressure decreases from 3 Pa to 0.03 Pa. This is

similar to the trend visible in the work by *Cahoy et al.* [2006, Figure 10c], who reported on the vertical structure of a wave-3 disturbance in atmospheric refractivity (proportional to neutral density) profiles obtained at 67.5°N–69.5°N, 2.76–2.79 hrs LST, L_s = 87°–92° in Mars Global Surveyor radio occultation profiles.

3. Discussion

[11] Three observations demonstrate that tidal and wave components of atmospheric dynamics at the season and latitude of the Phoenix atmospheric entry are not solely dominated by the diurnal migrating tide. Variations in the Phoenix surface pressure with time of day contain additional harmonic components beyond the diurnal component. MCS dayside temperature profiles exhibit a regular dependence on longitude. The vertical spacing of temperature extrema in the MCS profiles is greater than expected for the diurnal migrating tide.

[12] The MCS dayside temperature profiles, which are acquired in a fixed local time reference frame, exhibit variations in longitude that are dominated by a wave-3 harmonic. Two non-migrating tidal modes that previous studies [e.g., *Banfield et al.*, 2000; *Forbes et al.*, 2002; *Banfield et al.*, 2003; *Withers et al.*, 2003; *Angelats i Coll et al.*, 2004; *Cahoy et al.*, 2006] have identified in the martian atmosphere could be responsible. The first, dominated by diurnal Kelvin wave 2 or DK2, has a diurnal period (n = 1) and a true wavenumber of 2 (s = −2). The second, dominated by semi-diurnal Kelvin wave 1 or SK1, has a diurnal period (n = 2) and a true wavenumber of 1 (s = −1). As discussed by *Forbes et al.* [2002] and *Read and Lewis* [2004, pp. 124–125], the non-migrating DK2 mode can be produced by the interaction of the migrating diurnal tide and wave-3 longitudinal variations in planetary topography. Although it has a wavenumber of 2 to an observer at a fixed longitude, it produces wave-3 variations with longitude in the fixed local time frame of the MCS observations. The SK1 mode is produced similarly. Either or both of two non-migrating tidal modes, DK2 and SK1, could cause longitudinal variations. They will cause different relationships between the dayside and nightside MCS profiles. DK2 is more confined to the tropics than SK1, which tends to favour SK1 as the dominant non-migrating tidal mode responsible for the variations in Figure 1d. DK2 has a vertical wavelength of 10 scale heights and SK1, which is evanescent, has a vertical wavelength of 14 scale heights [*Withers et al.*, 2003]. In isolation, each of these modes has too long a vertical wavelength to cause the oscillations in Figure 1. Yet the interference of the diurnal migrating tide and these two non-migrating tides has the potential to create complex dependences on altitude, longitude and LST.

[13] A stationary wave with s = 3 could also contribute, although it is unlikely to propagate sufficiently high to play a major role [*Hollingsworth and Barnes*, 1996; *Angelats i Coll et al.*, 2004]. Traveling waves could also be present. Previous work at these latitudes using observations distributed over several weeks has identified the presence of traveling waves with a range of periods that are not simply related to the length of the martian day and a range of integer wavenumbers [*Wilson et al.*, 2002; *Hinson and Wang*, 2010]. Our use of 20 days of MCS observations in Figure 1d should minimize their contributions to our interpretations. Comprehensive interpretation of nightside MCS profiles, dayside MCS profiles, the Phoenix entry profile with its unusual range in longitude and local time, and Phoenix surface pressure measurements requires the application of a 3-D general circulation model that encompasses all longitudes and local times.

4. Conclusions

[14] The Phoenix entry profile contains large oscillations in temperature with each extremum separated by about 10 km. This separation is consistent with the vertical wavelength of the diurnal migrating tide. However, the strong wave-3 variations with longitude in dayside MCS temperature profiles show that the diurnal migrating tide is not the only periodic atmospheric disturbance present in the atmosphere during the Phoenix entry. The DK2 and SK1 non-migrating tidal modes could be responsible for this dependence on longitude.

[15] **Acknowledgments.** PW acknowledges support from NASA (NNX09AG16G) and discussions with David Kass and Armin Kleinbohl. DC acknowledges past support from the UK Science and Technology Facilities Council (STFC) awarded to the University of Bristol for Phoenix lander data reduction. PW and DC also acknowledge several reviewers and help and assistance from many people associated with the Phoenix project.

References

Angelats i Coll, M., F. Forget, M. A. López-Valverde, P. L. Read, and S. R. Lewis (2004), Upper atmosphere of Mars up to 120 km: Mars Global Surveyor accelerometer data analysis with the LMD general circulation model, *J. Geophys. Res.*, *109*, E01011, doi:10.1029/2003JE002163.

Banfield, D., B. Conrath, J. C. Pearl, M. D. Smith, and P. Christensen (2000), Thermal tides and stationary waves on Mars as revealed by Mars Global Surveyor Thermal Emission Spectrometer, *J. Geophys. Res.*, *105*, 9521–9537, doi:10.1029/1999JE001161.

Banfield, D., B. J. Conrath, M. D. Smith, P. Christensen, and R. J. Wilson (2003), Forced waves in the martian atmosphere from MGS TES nadir data, *Icarus*, *161*, 319–345.

Cahoy, K. L., D. P. Hinson, and G. L. Tyler (2006), Radio science measurements of atmospheric refractivity with Mars Global Surveyor, *J. Geophys. Res.*, *111*, E05003, doi:10.1029/2005JE002634.

Chapman, S., and R. Lindzen (1970), *Atmospheric Tides: Thermal and Gravitational*, Gordon and Breach, New York.

Forbes, J. F. (1995), Tidal and planetary waves, in *The Upper Mesosphere and Lower Thermosphere: A Review of Experiment and Theory*, *Geophys. Monogr. Ser.*, vol. 87, edited by R. M. Johnson and T. L. Killeen, pp. 67–87, AGU, Washington, D. C.

Forbes, J. M., A. F. C. Bridger, S. W. Bougher, M. E. Hagan, J. L. Hollingsworth, G. M. Keating, and J. Murphy (2002), Nonmigrating tides in the thermosphere of Mars, *J. Geophys. Res.*, *107*(E11), 5113, doi:10.1029/2001JE001582.

Hinson, D. P., and H. Wang (2010), Further observations of regional dust storms and baroclinic eddies in the northern hemisphere of Mars, *Icarus*, *206*, 290–305, doi:10.1016/j.icarus.2009.08.019.

Hollingsworth, J. L., and J. R. Barnes (1996), Forced stationary planetary waves in Mars's winter atmosphere., *J. Atmos. Sci.*, *53*, 428–448, doi:10.1175/1520-0469(1996)053.

Kleinböhl, A., et al. (2009), Mars Climate Sounder limb profile retrieval of atmospheric temperature, pressure, and dust and water ice opacity, *J. Geophys. Res.*, *114*, E10006, doi:10.1029/2009JE003358.

Lee, C., et al. (2009), Thermal tides in the Martian middle atmosphere as seen by the Mars Climate Sounder, *J. Geophys. Res.*, *114*, E03005, doi:10.1029/2008JE003285.

Leovy, C. B. (2001), Weather and climate on Mars, *Nature*, *412*, 245–249.

Magalhães, J. A., J. T. Schofield, and A. Seiff (1999), Results of the Mars Pathfinder atmospheric structure investigation, *J. Geophys. Res.*, *104*, 8943–8955.

McCleese, D. J., J. T. Schofield, F. W. Taylor, S. B. Calcutt, M. C. Foote, D. M. Kass, C. B. Leovy, D. A. Paige, P. L. Read, and R. W. Zurek (2007), Mars Climate Sounder: An investigation of thermal and water vapor structure, dust and condensate distributions in the atmosphere,

and energy balance of the polar regions, *J. Geophys. Res.*, *112*, E05S06, doi:10.1029/2006JE002790.

Read, P. L., and S. R. Lewis (2004), *The Martian Climate Revisited*, Springer, Berlin.

Smith, D., G. Neumann, R. E. Arvidson, E. A. Guinness, and S. Slavney (2003), Mars Global Surveyor Laser Altimeter Mission Experiment Gridded Data Record, *MGS-M-MOLA-5-MEGDR-L3-V1.0*, NASA Planet. Data Syst., Washington, D. C.

Smith, P. H., et al. (2009), H_2O at the Phoenix landing site, *Science*, *325*, 58–61, doi:10.1126/science.1172339.

Taylor, P. A., et al. (2010), On pressure measurement and seasonal pressure variations during the Phoenix mission, *J. Geophys. Res.*, *115*, E00E15, doi:10.1029/2009JE003422.

Wilson, R. J., and K. Hamilton (1996), Comprehensive model simulation of thermal tides in the Martian atmosphere, *J. Atmos. Sci.*, *43*, 1290–1326.

Wilson, R. J., D. Banfield, B. J. Conrath, and M. D. Smith (2002), Traveling waves in the northern hemisphere of Mars, *Geophys. Res. Lett.*, *29* (14), 1684, doi:10.1029/2002GL014866.

Withers, P., S. W. Bougher, and G. M. Keating (2003), The effects of topographically-controlled thermal tides in the Martian upper atmosphere as seen by the MGS accelerometer, *Icarus*, *164*, 14–32, doi:10.1016/S0019-1035(03)00135-0.

Withers, P., D. C. Catling, and J. R. Murphy (2010), Phoenix Lander Atmospheric Stucture Reduced Data Records, version 1.0, *PHX-M-ASE-5-EDL-RDR-V1.0*, NASA Planet. Data Syst., Washington, D. C.

Zurek, R. W. (1976), Diurnal tide in the Martian atmosphere, *J. Atmos. Sci.*, *33*, 321–337.

Zurek, R. W., J. R. Barnes, R. M. Haberle, J. B. Pollack, J. E. Tillman, and C. B. Leovy (1992), Dynamics of the atmosphere of Mars, in *Mars*, edited by H. H. Kieffer et al., pp. 835–933, Univ. of Ariz. Press, Tucson.

D. C. Catling, Department of Earth and Space Sciences, University of Washington, Box 351310, Seattle, WA 98195-1310, USA.

P. Withers, Center for Space Physics, Boston University, 725 Commonwealth Ave., Boston, MA 02215, USA. (withers@bu.edu)